water

MDPI

Article

Optimization of Scale Inhibitor Addition Scheme and Control of Phosphorus Content in External Cooling System of Synchronous Condenser

Xiantao Gu [1,*], Yuquan Wu [2], Yunqing Xu [2], Hongwei Zhao [2], Lin Yang [2], Xiaochun Chen [1], Peipei Fan [3], Junjie Zhang [3], Zhikui Liu [3], Tao Zhu [3], Yuxiang Gao [1] and Haosheng Dong [3]

[1] State Grid Anhui Electric Power Research Institute, Hefei 230601, China
[2] School of Materials Science and Engineering, Tianjin University, Tianjin 300350, China
[3] Extra High Voltage Branch, State Grid Anhui Electric Power Company, Hefei 230041, China
[*] Correspondence: guxt5619@163.com

Abstract: Scaling is one of the common problems in circulating cooling water systems, which can significantly affect the cooling efficiency of equipment in severe cases. At present, the problem of scaling is usually controlled by adding water treatment agents. However, taking the external cooling system of the synchronous condenser in an ultra-high-voltage converter station as an example, due to the lack of scientific understanding of scale inhibitors, there is often a problem of excessive dosing, resulting in unsatisfactory scale inhibition effects and difficulties in wastewater treatment and discharge. In addition, the extensive use of phosphorus-containing agents has led to the enrichment of phosphorus elements in water bodies. Therefore, the optimal amount of AS-582 scale inhibitor used in the converter station with the best scale inhibition effect was determined through static calcium carbonate deposition experiments, with the scale inhibition rate of 91.4% at 90 mg/L. And the scale inhibition mechanism was explored, where the lattice distortion mechanism and threshold effect play important roles. The AS-582 scale inhibitor was mixed with two green scale inhibitors, PASP and PESA, to obtain a phosphorus reduction formula that combined excellent scale inhibition performance and low phosphorus content. When using the optimal composite scale inhibitor of *n*(AS-582):*n*(PASP):*n*(PESA) = 4:1:1, the scale inhibition rate is 91.8% and the phosphorus content is reduced by one-third. The effectiveness of the formula was tested using dynamic circulating water experimental equipment under practical application conditions, proving its practical value.

Keywords: recirculating cooling water system; scaling resistance performance; phosphorus content; dynamic corrosion and scale inhibition experiment

check for updates

Academic Editor: Christos S. Akratos

Received: 4 December 2024
Revised: 21 January 2025
Accepted: 22 January 2025
Published: 2 February 2025

Citation: Gu, X.; Wu, Y.; Xu, Y.; Zhao, H.; Yang, L.; Chen, X.; Fan, P.; Zhang, J.; Liu, Z.; Zhu, T.; et al. Optimization of Scale Inhibitor Addition Scheme and Control of Phosphorus Content in External Cooling System of Synchronous Condenser. *Water* **2025**, *17*, 415. https://doi.org/10.3390/w17030415

1. Introduction

Freshwater resources, as a fundamental natural resource, play a critical role in maintaining ecological stability and are considered a strategic economic asset for nations [1]. With the rapid advancement of the global economy, the demand for industrial water is steadily rising. This trend is particularly pronounced in China, where industrial water accounts for nearly half of all non-agricultural water consumption [2]. Cooling water constitutes a significant portion of industrial water usage, making it essential to enhance the efficiency of industrial cooling water utilization. Synchronous condensers are vital reactive power compensation devices in ultra-high-voltage direct current (UHVDC) transmission systems, and their operational stability directly impacts the stability of the power grid [3,4]. As power systems continue to expand in scale and complexity, the capacity of individual synchronous condensers has increased accordingly [5]. However, large-capacity synchronous condensers generate substantial heat during operation, and if not promptly cooled, overheating may occur, potentially resulting in shutdowns [6]. Taking the external cooling water system of a UHVDC converter station's synchronous condenser as an example, this system uses an open-loop recirculating cooling method. While this approach significantly improves water resource utilization, it also causes increasing ion concentration in the cooling water due to successive cycles, eventually reaching supersaturation and forming insoluble salts. These salts then deposit on the surfaces within the cooling system, resulting in scale formation [7,8]. The presence of scales severely impairs the cooling efficiency of the external cooling water system, diminishing the condenser's cooling efficacy.

The main methods for addressing scaling in recirculating cooling water systems include chemical treatment methods [9,10], magnetization and electromagnetic methods [11], ultrasonic methods [12], and electrochemical descaling [13,14]. Among these, the addition of scale inhibitors is considered the most economical and efficient solution and is widely used in various recirculating cooling water systems. Currently, the converter station employs AS-582 as its scale inhibitor due to its low cost, good scale inhibition performance, and relatively low phosphonate content (6.0%) [15]. However, due to the lack of a precise understanding of optimal dosing requirements, over-dosing or frequent dosing often occurs, resulting in suboptimal scale inhibition and challenges in wastewater treatment and discharge. Additionally, the excessive use of AS-582 can lead to phosphorus accumulation, potentially triggering the overgrowth of bacteria and algae, which adversely affects the cooling water system's performance and further degrades water quality. Wastewater management is a critical factor in achieving green and sustainable practices [16]. Thus, reducing or eliminating phosphorus in recirculating cooling systems is essential, and the use of green polymer-based scale inhibitors presents an effective solution. Artificially synthesized polyaspartic acid (PASP) and polyepoxysuccinic acid (PESA) are the most typical green polymer scale inhibitors, which contain a large number of carboxyl and ether groups in the structure. They can achieve scale inhibition by chelating calcium ions or inducing the lattice distortion of calcium carbonate crystals. At the same time, they have excellent environmental friendliness and biodegradability [17,18]. However, green polymer scale inhibitors usually have the disadvantage that their scale inhibition performance is greatly affected by calcium ion concentration or temperature. When added alone, it is often difficult to adapt to practical applications under complex conditions [19–21]. Compared to one single scale inhibitor, there is usually a synergistic effect between composite scale inhibitors, which can effectively inhibit the formation of scale [22]. In addition, combining efficient scale inhibitors suitable for complex environments with green polymer scale inhibitors can effectively reduce the phosphorus content in water caused by scale inhibitors while ensuring scale inhibition performance. Long et al. developed an efficient and environmentally friendly composite scale inhibitor using PESA and sodium carboxymethyl cellulose (CMC-Na) as raw materials [23]. After adding it to water, the $CaCO_3$ scale undergoes lattice distortion, resulting in a decrease in grain size and crystallinity, achieving the purpose of scale inhibition. Ou et al. investigated the synergistic effect of sodium gluconate (SG) and 2-phosphonobutane-1,2,4-tricarboxylic acid (PBTC) in inhibiting the formation of $CaCO_3$. While effectively reducing the phosphate content of the scale inhibitor, the particular inhibition mechanism of $CaCO_3$ scaling was completely different from PBTC [24]. Because SG can recognize positively charged calcium ions and react with them to form stable soluble calcium complexes, they slow down the germination rate of $CaCO_3$ scaling by 4.3 times.

In addition, most of the current evaluations of the scale inhibition performance of scale inhibitors are still in the static experimental stage, making it difficult to determine the performance of scale inhibitors under complex water quality and dynamic circulation conditions. In this study, performance tests were initially conducted on the AS-582 scale inhibitor currently used at the converter station, along with two green polymer-based inhibitors (PESA and PASP), to determine the optimal dosage for maximum scaling prevention and to investigate their inhibition mechanisms, mainly including the lattice distortion and the threshold effect. Next, a mixed inhibitor was formulated by combining AS-582 with PESA and PASP, exploring the optimal ratio to achieve effective scaling inhibition while reducing the phosphorus content of the inhibitor. Finally, dynamic circulating water experimental equipment was employed in the laboratory to simulate real-world conditions, assessing both the corrosion inhibition and scaling resistance performance of the reduced phosphorus formulation as well as its effectiveness in lowering phosphorus levels in the cooling water system.

2. Experiment

2.1. Instruments and Reagents

Instruments: D8 Advance X-ray diffractometer (Bruker, Berlin, Germany), S-4800 scanning electron microscope (Hitachi, Tokyo, Japan).

Reagents: anhydrous calcium chloride (analytical grade, Tianjin Heowns, Tianjin, China); disodium ethylenediaminetetraacetate dihydrate (analytical grade, Tianjin Heowns); disodium tetraborate decahydrate (analytical grade, Tianjin Heowns); calcium carboxylate (analytical grade, Tianjin Heowns); potassium chloride (analytical grade, Tianjin Heowns); calcium hydroxide (analytical grade, Tianjin Jiangtian Chemical, Tianjin, China); potassium hydroxide (analytical grade, Tianjin Jiangtian Chemical); sodium bicarbonate (analytical grade, Tianjin Jiangtian Chemical); polyaspartic acid (PASP, $C_4H_5NO_3M(C_4H_4NO_3M)_m(C_4H_4NO_3M)_nC_4H_4NO_3M_2$, molecular mass 1000~5000 Da, 90%, Shandong Yousuo Chemical, Linyi, China); polyepoxysuccinic acid (PESA, $HO(C_4H_2O_5M_2)_nH$, molecular mass 400~1500 Da, 90%, Shandong Yousuo Chemical); AS-582 scale inhibitor solution (Acrylic Acid-2-Acrylamido-2-Methylpropane Sulfonic Acid Copolymer (AA/AMPS), 1-Hydroxy Ethylidene-1,1-Diphosphonic Acid (HEDP), 2-Phosphonobutane-1,2,4-Tricarboxylic Acid (PBTCA), solid content 12.8%, Shandong Zhongjiang, Jinan, China).

The Preparation of Calcium Carboxylate Indicator: weigh 0.2 g of calcium carboxylate powder, mix and grind evenly with 100 g of potassium chloride, and store in a ground-glass stoppered bottle.

The Preparation of EDTA Solution: weigh 3.7224 g of disodium ethylenediaminetetraacetate dihydrate, dissolve in deionized water in a beaker, and transfer to a 1000 mL volumetric flask for constant volume.

2.2. Static Scale Inhibition Experiment

Using the static calcium carbonate deposition method, experiments were conducted with deionized water and the make-up water from the cooling system of the converter station's synchronous condenser (hereafter referred to as "make-up water") as test waters. We added 250 mL of test water to a 500 mL volumetric flask and used a burette to add a certain volume of calcium chloride standard solution. A specified amount of scale inhibitor solution was added and thoroughly mixed. Then, we added 20 mL borax buffer solution (3.8 g/L). Slowly, we added a certain volume of sodium bicarbonate standard solution using a burette (shake while adding). We diluted this with water to the mark and shook well. The concentration of Ca^{2+} was 220 mg/L and the concentration of HCO_3^- was 732 mg/L. The pH of the test solution was ~9. The flasks were incubated in a water bath at 80 °C for 10 h. After this incubation period, the upper clear solution was filtered while hot, and an aliquot of the filtrate was taken. The calcium carboxylate indicator and buffer solution (200 g/L KOH solution) were then added to the filtrate. The remaining Ca^{2+} concentration in the filtrate was measured using EDTA complexometric titration. The scale inhibition rate was calculated using the following formula:

$$\eta_s = \frac{C_1 - C_0}{C_2 - C_0} \times 100\% \quad (1)$$

where η_s is the scale inhibition rate (%), C_0 is the concentration of Ca^{2+} in the filtrate without the scale inhibitor (mg/L), C_1 is the concentration of Ca^{2+} in the filtrate with the scale inhibitor (mg/L), and C_2 is the initial concentration of Ca^{2+} in the prepared water sample (mg/L).

All values related to the dosage of scale inhibitors are the solid mass of scale inhibitors.

2.3. Dynamic Scale Inhibition and Corrosion Inhibition Test

The dynamic circulating water experimental apparatus, as shown in Figure 1, was used to simulate the actual operating process of the external cooling system of a synchronous condenser in a laboratory. By adding $CuCl_2$ and $NaHCO_3$ to groundwater (total alkalinity 43.5 mg/L, calcium hardness 102.5 mg/L, and total hardness 142.5 mg/L), the water quality of the external cooling system of synchronous condenser (total alkalinity 115.5 mg/L, calcium hardness 154.4 mg/L, and total hardness 191.5 mg/L) was simulated. During the dynamic cycle, the cooling water continuously evaporated and concentrated, and the conductivity (i.e., ion concentration) increased. The apparatus was equipped with probes that monitored parameters such as conductivity, the thermal resistance of scale, and the corrosion rate of carbon steel.

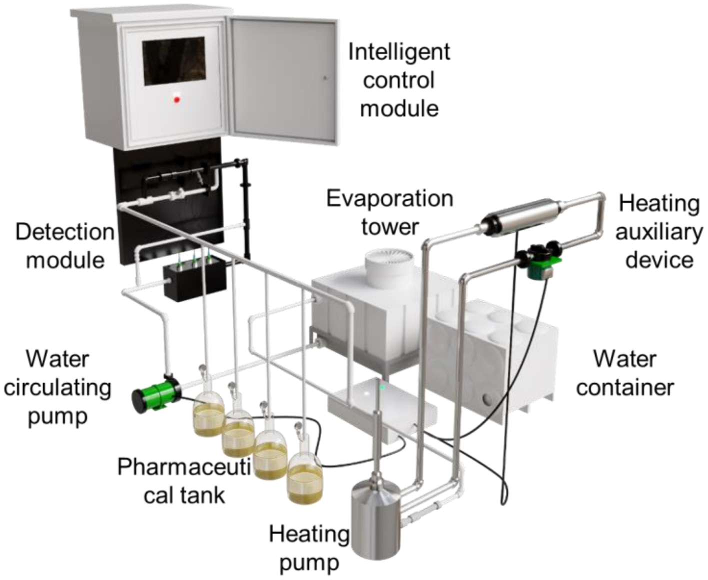

Figure 1. Schematic diagram of the dynamic circulating water experimental apparatus.

3. Results and Discussion

3.1. Performance Testing of AS-582 as a Scale Inhibitor

In previous studies, the scale inhibition performance of AS-582 was briefly evaluated, but the scale inhibition performance under different water quality conditions and the scale inhibition mechanism were lacking [15]. Therefore, using deionized water and the cooling water supplement from the converter station synchronous condenser (hereinafter referred to as "supplement water") as experimental water, static calcium carbonate deposition tests were conducted on the scale inhibitor AS-582 at various dosages. The scale inhibition performance is shown in Figure 2.

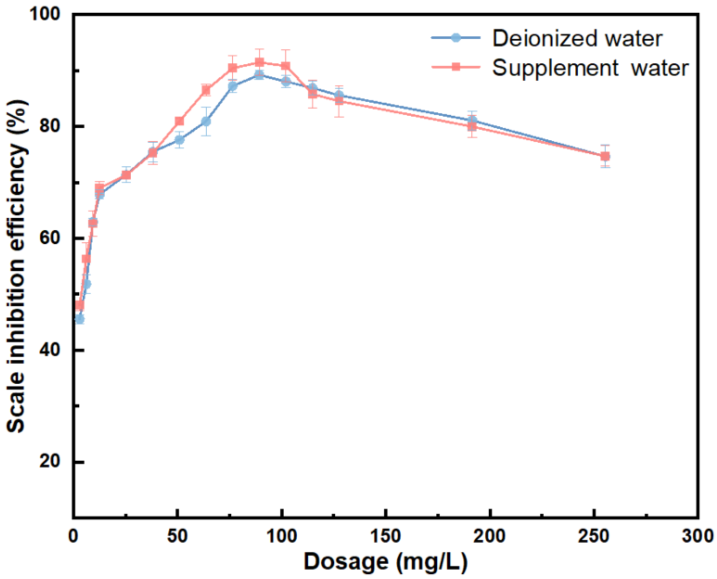

Figure 2. Variation in scale inhibition rate with dosage in two water samples.

As shown in Figure 2, the scale inhibition performance of the inhibitor AS-582 does not exhibit significant differences between the deionized water sample and the supplement water sample, with both curves displaying a similar trend. When the dosage is low (1–15 mg/L), the scale inhibition rate increases rapidly with the increase in dosage. In the deionized water sample, the scale inhibition rate rises from 47.9% to 68.9%, while in the make-up water sample, it increases from 46.4% to 67.8%. As the dosage is further increased (15–90 mg/L), the growth of the scale inhibition rate slows down. At the dosage of 90 mg/L, the scale inhibition rates reach the maximum values of 91.4% and 89.1% for the two water samples, respectively. When the dosage exceeds 90 mg/L, the scale inhibition rates first remain stable with the increase in scale inhibitor dosage and then decrease when the dosage is too high. The rapid response of the scale inhibition effect to the dosage and the ability to maintain stability around the optimal dosage indicate the existence of a significant "threshold effect" [25]. The mechanism of scale inhibitors is to affect crystal nucleation and hinder crystal growth by adsorbing on heterogeneous nucleation centers or active sites of calcium carbonate crystals [26,27]. Therefore, adding trace amounts of scale inhibitors can significantly reduce the precipitation of calcium carbonate scale. However, due to the limited number of nucleation centers or active sites, the scale inhibition effect no longer improves when the dosage reaches the optimal level. And when the dosage exceeds a certain value, the scale inhibition effect will actually decrease, which is consistent with the phenomenon of the excessive addition of scale inhibitors with the unsatisfactory scale inhibition effect that occurs in the converter station. This may be due to the limited adsorption sites on the crystal surface. When excessive scale inhibitors are added, the excess scale inhibitor molecules present in the water will alter the properties of the aqueous solution and the crystallization behavior of $CaCO_3$, leading to the occurrence of side reactions and an increase in precipitation. Therefore, when using scale inhibitors, the dosage should be accurately controlled to achieve the most ideal scale inhibition effect to reduce the dosage and cost.

3.2. Analysis of AS-582 Scale Inhibition Mechanism

Calcium carbonate has three common crystalline forms: calcite, aragonite, and vaterite. From a thermodynamic stability perspective, calcite is the most stable, while vaterite, which exists in a metastable state, is the least stable, and aragonite lies in between [28]. Therefore, when the crystal form of calcium carbonate scale is mainly cubic calcite or strip-shaped aragonite, its structure is compact and its texture is hard. When the main crystal form of calcium carbonate scale is vaterite, its structure is loose and porous, and it is difficult to grow. These irregular spherical crystals are often suspended in water [20]. After conducting static calcium carbonate deposition tests, the calcium carbonate scales were collected and characterized for their phase composition and microstructure using X-ray diffraction (XRD) and scanning electron microscopy (SEM).

Figure 3 shows the XRD patterns of the calcium carbonate scales obtained under different inhibitor dosages. In the XRD pattern of the calcium carbonate scale obtained without any inhibitor, peaks at 29.56°, 47.66°, and 48.62° can be attributed to the (1 0 4), (0 1 8), and (1 1 6) planes of the calcite crystalline form. Additionally, peaks at 26.42°, 27.38°, and 46.08° can be attributed to the aragonite crystalline form, indicating that the scale primarily consists of calcite, with a small amount of aragonite present [29]. After the addition of the scale inhibitor, the XRD pattern of the calcium carbonate scale exhibited significant changes, with diffraction peaks at 25.02°, 27.22°, and 32.88° corresponding to the (0 1 1), (1 2 0), and (2 1 1) planes of the vaterite crystalline form. It is also observed that as the dosage of the scale inhibitor increases, the intensity of the calcite peaks gradually weakens, while the intensity of the vaterite peaks gradually strengthens [30].

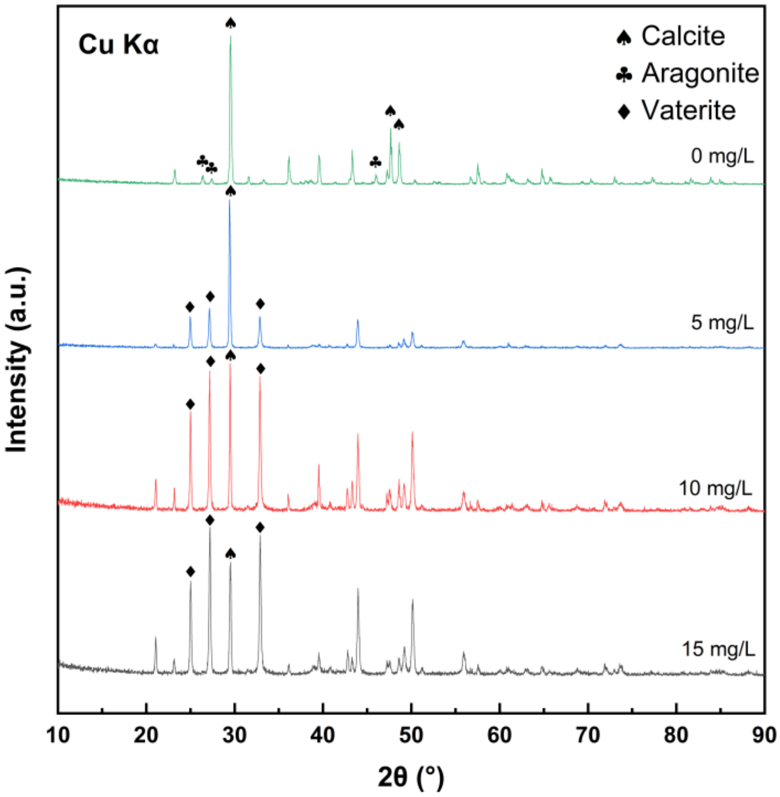

Figure 3. XRD patterns of calcium carbonate scale samples at AS-582 dosing amounts of 0, 5, 10, and 15 mg/L.

To further clarify the phase composition of calcium carbonate scale samples at different dosing amounts of the scale inhibitor, a simple, quick, and less error-prone quantitative analysis method was referenced [31]. Specifically, the relative content of each phase in the calcium carbonate scale was estimated based on the peak values of specific crystal planes in the XRD spectra. The quantitative calculation Formulas (2) and (3) are applicable for the calcite (C)-aragonite (A) system, while Formulas (4) and (5) are applicable for the calcite (C)-vaterite (V) system.

$$C\% = I_C/(I_C + 3.5530 I_A) \times 100\% \tag{2}$$

$$A\% = I_A/(I_A + 0.2874 I_C) \times 100\% \tag{3}$$

$$C\% = I_C/(I_C + 10.0058 I_V) \times 100\% \tag{4}$$

$$V\% = I_V/(I_V + 0.1025 I_C) \times 100\% \tag{5}$$

The calculation results are shown in Table 1.

Table 1. Relative content of each phase in calcium carbonate scale samples at different dosing amounts of scale inhibitor.

Dosing (mg/L)	Calcite (wt.%)	Aragonite (wt.%)	Vaterite (wt.%)	Others (wt.%)
0	81.6	18.1	–	0.3
5	24.6	–	74.9	0.5
10	12.9	–	86.9	0.3
15	10.7	–	89.1	0.2

Based on Table 1, it can be observed that in the blank group without the addition of a scale inhibitor, the primary crystalline form of calcium carbonate is calcite, which constitutes as much as 81.6%, while aragonite accounts for 18.1%. After the addition of the AS-582 scale inhibitor, the relative content of calcite significantly decreases and aragonite essentially disappears, while the relative content of vaterite notably increases. At dosage of 15 mg/L of the scale inhibitor, the relative content of vaterite reaches 89.1%.

The SEM images in Figure 4a,b reveal that the calcium carbonate scale obtained without the addition of a scale inhibitor primarily consists of regular, densely packed hexagonal structures, measuring between 10 and 20 µm. This is characteristic of the calcite structure. Once calcium carbonate nucleates and grows in the form in the circulating water system, its hardness and smooth surface firmly adhere to the walls, making removal difficult [29]. Additionally, a few granular and elongated structures can be observed, corroborating the presence of a small amount of aragonite as indicated by the XRD. In contrast, the morphology of the calcium carbonate scale under the condition of adding 15 mg/L of scale inhibitor is shown in Figure 4c,d. It is almost impossible to observe the hexagonal structure, mainly consisting of irregular, small-volume, and loosely packed ellipsoidal structures, which are typical of vaterite structures [30].

According to the lattice distortion theory, scale inhibitor molecules can selectively adsorb on the active sites of crystals, hindering the growth and "dissolution recrystallization" of metastable vaterite, ultimately leading to its transformation into stable calcite, and forming loose structured calcium carbonate particles mainly composed of vaterite. In addition, the phosphonic acid, carboxylic acid and other functional groups present in AS-582 scale inhibitor bond with Ca^{2+} to form stable soluble chelate molecules, thereby increasing the solubility of Ca^{2+} in water and hindering the precipitation of calcium carbonate.

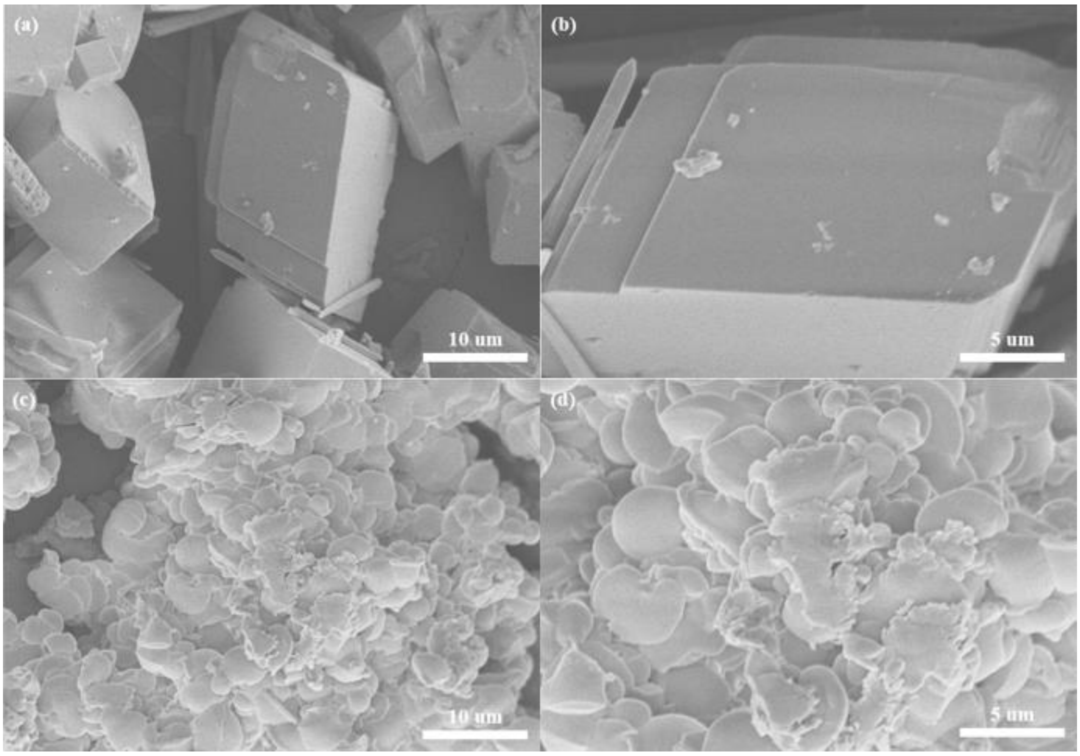

Figure 4. SEM images of calcium carbonate scale samples before and after the addition of scale inhibitor: (**a**,**b**) without scale inhibitor; (**c**,**d**) with a scale inhibitor addition of 15 mg/L.

3.3. Testing of Scale Inhibition Performance of PESA and PASP

Using deionized water as the experimental medium, static calcium carbonate deposition tests were conducted for the green polymer scale inhibitors PESA and PASP at varying dosages. The results of the scale inhibition performance are presented in Figure 5. The trends observed for the scale inhibition performance of both green polymer inhibitors are similar to that of AS-582, characterized by an initial rapid increase followed by a gradual flattening, and finally a decreasing trend at excessive dosage. For PASP, the scale inhibition rate curve displays a relatively gentle slope, with a peak inhibition rate of 46.9% occurring at a dosage of 40 mg/L. In contrast, PESA exhibits a more pronounced increase in the scale inhibition rate within the low dosage range of 1–10 mg/L, rising from 13.3% at 1 mg/L to 64.0% at 15 mg/L. As the dosage continues to increase, the rate of scale inhibition growth slows, reaching a maximum of 72.3% at a dosage of 30 mg/L. It is noteworthy that both PESA and PASP have a significant “threshold effect”, and the maximum scale inhibition rate does not exceed 80%, far lower than the 91.4% of AS-582. Overall, the scale inhibition effectiveness can be ranked as follows: AS-582 > PESA > PASP.

The XRD spectra of calcium carbonate scale samples obtained after adding the two green polymer scale inhibitors are shown in Figure 6, with a dosage of 100 mg/L for both inhibitors. In the XRD patterns of the two calcium carbonate scale samples, the peak intensity corresponding to the calcite crystal phase is relatively weakened, particularly in the calcium carbonate scale sample obtained after adding PESA, where the calcite crystal phase is nearly absent. This indicates that both green polymer scale inhibitors exhibit a scale inhibition mechanism similar to AS-582, namely the lattice distortion mechanism. By mixing these three inhibitors, it is expected to produce a synergistic effect to achieve better scale inhibition while reducing phosphorus content in water.

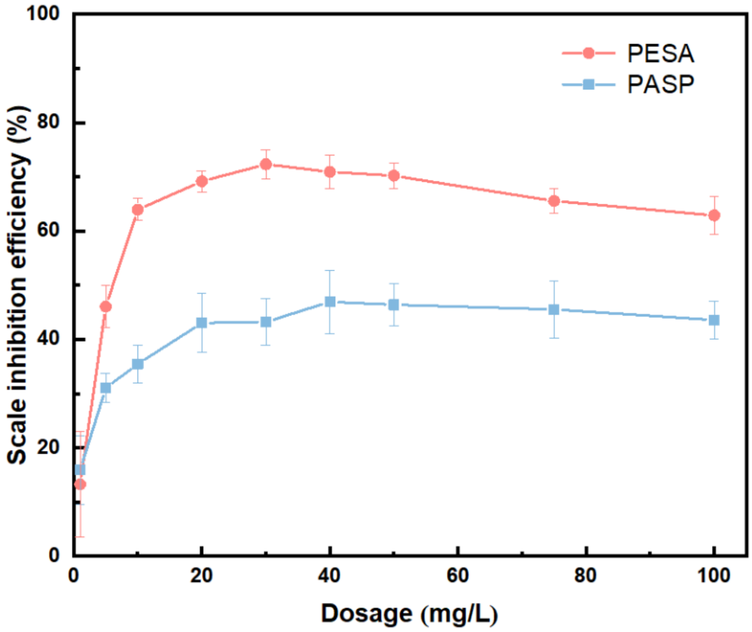

Figure 5. Variation in scale inhibition rates of two green polymer inhibitors, PESA and PASP, with dosage.

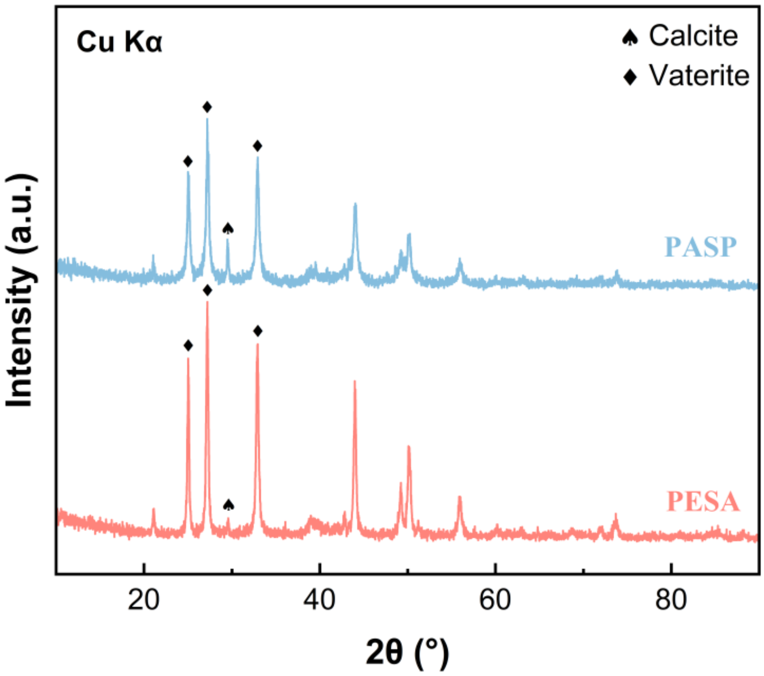

Figure 6. XRD patterns of calcium carbonate scale samples obtained after the addition of two green polymer scale inhibitors.

3.4. Scale Inhibition Performance Testing of Mixed Inhibitors

Using the currently employed AS-582 as the main component, two green polymer scale inhibitors, PESA and PASP, were formulated as auxiliary components in varying ratios to create mixed-scale inhibitors. The scale inhibition effectiveness was tested in the make-up water, with results shown in Table 2.

Table 2. Scale inhibition performance of various inhibitors at different addition amounts.

AS-582 (mg/L)	PASP (mg/L)	PESA (mg/L)	Formulation Ratios	Scale Inhibition Rate (%)
90	0	0	1:0:0	92.3
90	45	0	2:1:0	89.7
90	0	45	2:0:1	89.2
80	10	0	8:1:0	91.3
80	0	10	8:0:1	90.2
80	5	5	16:1:1	91.3
60	15	15	4:1:1	91.8
45	45	0	1:1:0	90.2
45	27.5	27.5	2:1:1	85.5
30	30	30	1:1:1	83.9

When the addition of AS-582 was maintained at an optimal dosage of 90 mg/L for scale inhibition, the scale inhibition rates decreased to varying degrees upon the addition of PASP and PESA. This indicates that the occurrence of the "threshold effect" is directly related to the total amount of scale inhibition functional groups present in the water. Therefore, the total addition of the mixed-scale inhibitors was controlled at 90 mg/L. For the mixed scale inhibitors, the optimal ratio for achieving the best scale inhibition effect was found to be n(AS-582):n(PASP):n(PESA) = 4:1:1, resulting in a scale inhibition rate of 91.8%. This suggests that by employing mixed-scale inhibitors, it is possible to achieve a reduction in phosphorus content in water by one-third while ensuring effective scale inhibition.

3.5. Dynamic Corrosion Inhibition and Scale Inhibition Experiments with Phosphorus Content Detection

In addition to excellent scale inhibition performance, the ability to provide effective corrosion inhibition in a circulating cooling water system is another important indicator for evaluating the rationality of water treatment chemical addition schemes. Therefore, dynamic circulating water experimental equipment was used to test the changes in fouling thermal resistance and the carbon steel corrosion rate under three conditions: no addition of corrosion scale inhibitors, the addition of 90 mg/L AS-582, and the addition of 90 mg/L mixed corrosion scale inhibitors (n(AS-582):n(PASP):n(PESA) = 4:1:1, referred to as the phosphorus reduction formulation) at ion concentrations of 6–15 times (concentration multiples, a conductivity of 1200–3000 μS/cm). The results are shown in Figure 7.

In terms of scale inhibition, the fouling thermal resistance did not show significant changes with increasing ion concentration, regardless of whether corrosion scale inhibitors were added. Compared to the scenario without any corrosion scale inhibitors, the fouling thermal resistance slightly decreased by about 5.0×10^{-5} m^2·K/W after adding 90 mg/L of AS-582. In contrast, the addition of 90 mg/L of the phosphorus reduction formulation resulted in a significant decrease in fouling thermal resistance, approximately by 1.3×10^{-4} m^2·K/W, which is only two-thirds of that observed without corrosion scale inhibitors. This indicates that the phosphorus reduction formulation exhibits superior scale inhibition performance in the simulated environment compared to the single formulation. In terms of corrosion inhibition, the carbon steel corrosion rate increased with rising ion concentrations, regardless of whether corrosion scale inhibitors were added. However, after adding corrosion scale inhibitors, the carbon steel corrosion rates at various ion concentrations decreased to some extent compared to the scenario without any addition. Notably, the phosphorus reduction formulation demonstrated a more significant effect, indicating that it can provide better corrosion inhibition in the simulated environment.

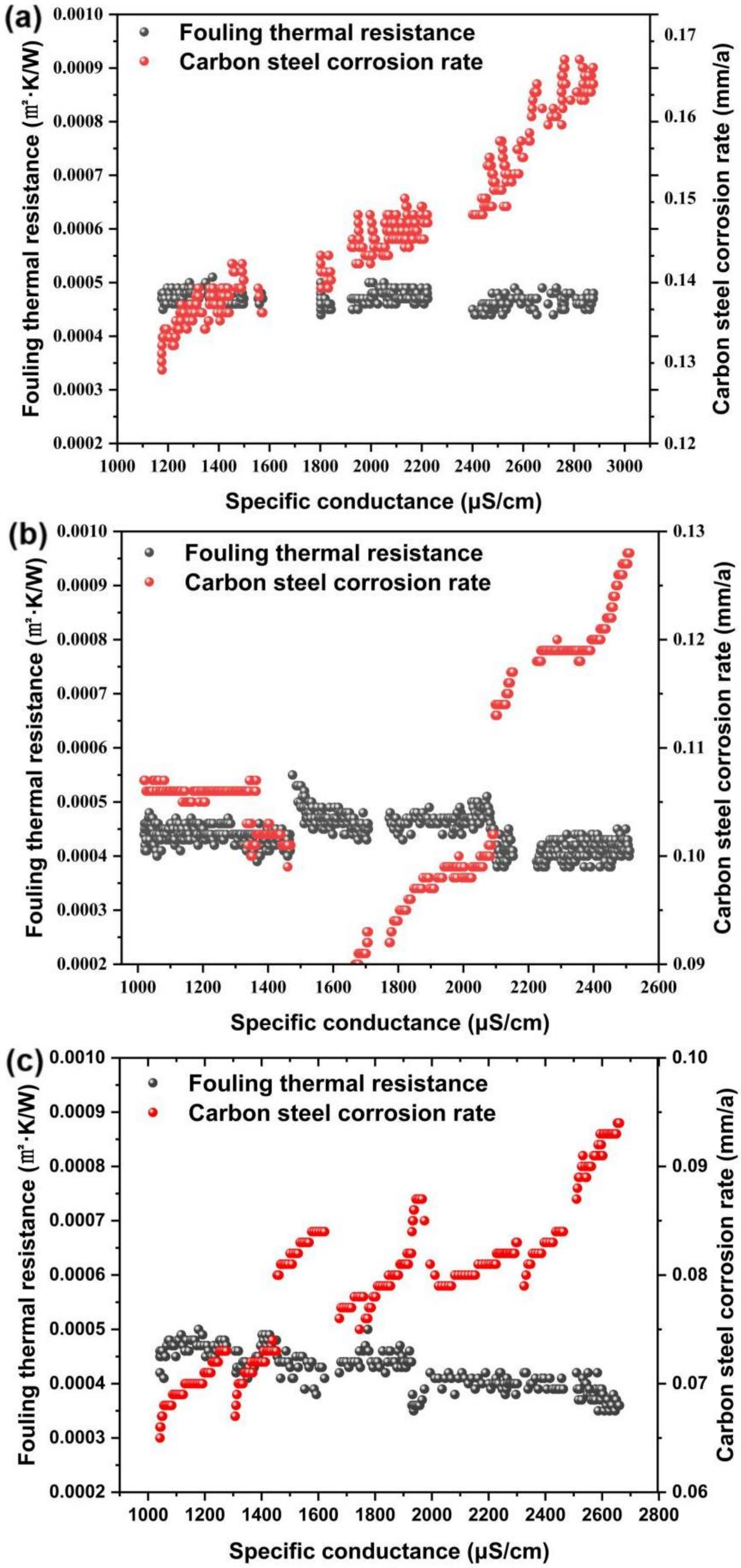

Figure 7. (**a**) Carbon steel corrosion rate and fouling thermal resistance at different ion concentrations without the addition of corrosion scale inhibitors. (**b**) With the addition of 90 mg/L AS-582. (**c**) With the addition of a 90 mg/L phosphorus reduction formulation.

To assess the effectiveness of the phosphorus reduction formulation in reducing phosphorus content in water bodies, the phosphorus levels in different water samples were measured, as shown in Table 3. Sample 1 corresponds to the onsite water sample from the external cooling system of the synchronous condenser (which has been using AS-582 for an extended period), while Sample 2 is the water sample concentrated thirteen times in the dynamic circulating water experimental equipment (initially treated with 90 mg/L of the phosphorus reduction formulation). Compared to Sample 1, both organic phosphorus and total phosphorus levels in Sample 2 showed a significant decrease, indicating that the rational use of the phosphorus reduction formulation can effectively alleviate the accumulation of phosphorus in the external cooling system of the synchronous condenser.

Table 3. Phosphorus content of each water sample (measured as PO_4^{3-}) (mg/L).

Number	Total Phosphorus	Organic Phosphorus	Orthophosphorus
1	6.0	5.7	0.4
2	2.3	2.1	0.2

4. Conclusions

The static calcium carbonate deposition experiments determined that AS-582 exhibits optimal scale inhibition performance at an addition amount of 90 mg/L, achieving a scale inhibition rate of 91.4%. With the addition of AS-582, the nucleation and "dissolution-recrystallization" of calcium carbonate crystals in the circulating cooling water system are inhibited, and the scale changes from calcite to the loose and porous small vaterite, thereby achieving the goal of scale inhibition. Furthermore, the optimal ratio for the combined use of AS-582 with the green polymer scale inhibitors PESA and PASP was identified as n(AS-582):n(PASP):n(PESA) = 4:1:1. Finally, dynamic corrosion inhibition and scale inhibition experiments demonstrated that the phosphorus reduction formulation can maintain excellent corrosion inhibition and scale inhibition effects under conditions close to practical applications, effectively reducing phosphorus content in the water of the external cooling system of the synchronous condenser. This not only helps ensure the safe and reliable operation of the synchronous condenser and the power grid but also aids in preventing water eutrophication, protecting water resources, and promoting the coordinated development of green industries.

Author Contributions: Validation, X.C.; formal analysis, X.G.; investigation, X.G., P.F., J.Z. and Z.L.; resources, X.G.; data curation, H.D.; writing—original draft preparation, X.G.; writing—review and editing, X.G. and L.Y.; visualization, Y.W., Y.X. and H.Z.; project administration, T.Z.; funding acquisition, Y.G. All authors have read and agreed to the published version of the manuscript.

Funding: This research was funded by State Grid Anhui Electric Power Research Institute Technology Project, grant number [B31205230008].

Data Availability Statement: The original contributions presented in the study are included in the article, and further inquiries can be directed to the corresponding author.

Conflicts of Interest: Authors Xian-Tao Gu, Xiao-Chun Chen, and Yu-Xiang Gao were employed by the State Grid Anhui Electric Power Research Institute; Authors Pei-Pei Fan, Jun-Jie Zhang, Zhi-Kui Liu, Tao Zhu, and Hao-Sheng Dong were employed by the State Grid Anhui Electric Power Company Extra High Voltage Branch. The remaining authors declare that the research was conducted in the absence of any commercial or financial relationships that could be construed as a potential conflict of interest.

References

1. Dudgeon, D.; Arthington, A.H.; Gessner, M.O.; Kawabata, Z.-I.; Knowler, D.J.; Lévêque, C.; Naiman, R.J.; Prieur-Richard, A.-H.; Soto, D.; Stiassny, M.L.J.; et al. Freshwater biodiversity: Importance, threats, status and conservation challenges. *Biol. Rev.* **2006**, *81*, 163–182. [CrossRef]
2. National Bureau of Statistics of China. *China Statistical Yearbook—2023*; China Statistics Press: Beijing, China, 2023.
3. Chubraeva, L.; Timofeev, S. Modern Reactive Power Generators. In Proceedings of the Actual Problem of Electromechanics and Electrotechnology, Yekaterinburg, Russia, 13–16 November 2017.
4. Igbinovia, F.O.; Fandi, G.; Muller, Z.; Tlusty, J. Reputation of the Synchronous Condenser Technology in Modern Power Grid. In Proceedings of the 2018 International Conference on Power System Technology (POWERCON), Guangzhou, China, 6–8 November 2018; Volume 313, p. 012006.
5. Ma, M.; Jiang, M.; Li, Y. Research on fault diagnosis method of turn to turn short circuit in rotor winding of large-scale dual water internal cooling condenser. *Electr. Mach. Control* **2021**, *25*, 19–27.
6. Wang, A.; Li, J.; Ma, Y.; Sun, F. Faults Analysis of Double Water Inner Cooled Synchronous Machines. In Proceedings of the 2019 IEEE International Conference on Prognostics and Health Management (ICPHM), San Francisco, CA, USA, 17–20 June 2019; pp. 6–7.
7. Ren, Z.; Yan, Y.; Yan, G.; Xu, B.; Zhou, W.; Zhou, T. Research on the Function and Key Technology of the Large-capacity Dual Internal Water Cooled Synchronous Condenser in UHVDC System. *High Volt. Eng.* **2019**, *45*, 1795–1802.
8. Li, G.; Niu, Z.; Xie, Q.; Zhen, J.; Xia, Z. Analysis of scaling causes and anti-scaling countermeasures of external cooling system of large-scale synchronous condenser in Northwest region of China. *Therm. Power Gener.* **2024**, *53*, 167–176.
9. Ma, W.; Liu, C.; Zhang, L.; Zhang, Y. Inhibition of calcium carbonate by low phosphorus copolymers rich in carboxylic acids. *J. Polym. Res.* **2023**, *30*, 148. [CrossRef]
10. Yang, J.; Hu, Z.; Wang, Z.; Wu, C.; Dong, L.; Meng, X.; Lin, X.; Zhao, J.; Chen, Y. Preparation and scale inhibition performance of modified polyaspartic acid (M-PASP). *J. Mol. Liq.* **2024**, *401*, 124712. [CrossRef]
11. Yang, Z.; Xiong, L.; Luo, Y.; Chen, J.; Miao, X.; Wu, Y. Experiment Research on the Frequency Effects of Pulsed Electromagnetic Field on Industrial Circulating Water. In Proceedings of the 2015 International Conference on Computer Science and Environmental Engineering (CSEE 2015), Beijing, China, 17 May 2015; pp. 373–382.
12. Oliveira, L.R.; Pereira, L.G.; Teixeira, L.D.; da Silva, M.V.; Pepe, I.M.; Ferreira, V.P.; Junior, L.C.; Demetino, G.G.; de Mattos, F.O.; Cordeiro, A.L.; et al. Calcium carbonate scaling control on heat plate exchange surfaces using ultrasound. *J. Braz. Soc. Mech. Sci. Eng.* **2024**, *46*, 109. [CrossRef]
13. Jiang, B.; Ren, X.; Liu, Q.; Yue, X.; Yang, Q.; Liu, Y.; Xu, H.; Zhou, J. Electrochemical water softening technology: From fundamental research to practical application. *Water Res.* **2024**, *250*, 121077. [CrossRef] [PubMed]
14. Xu, H.; Lei, J.; Yang, H.; Yan, W.; Yang, L. Checking on the treatment ability of electrochemical scale removing technology and its improvement. *Ind. Water Treat.* **2019**, *39*, 17–20.
15. Gu, X.; Xu, Y.; Wu, Y.; Zhang, L.; Zhang, J.; Chen, X.; Zhou, Z.; Fan, P.; Gao, Y.; Ji, Q.; et al. Water Quality Analysis of a 300 Mvar Large-Scale Dual Internal Water Cooling Synchronous Condenser External Cooling System and Exploration of Optimal Water Treatment Agent Dosage at Different Temperatures. *Water* **2024**, *16*, 3158. [CrossRef]
16. Obaideen, K.; Shehata, N.; Sayed, E.T.; Abdelkareem, M.A.; Mahmoud, M.S.; Olabi, A. The role of wastewater treatment in achieving sustainable development goals (SDGs) and sustainability guideline. *Energy Nexus* **2022**, *7*, 100112. [CrossRef]
17. Liu, D.; Dong, W.; Li, F.; Hui, F.; Lédion, J. Comparative performance of polyepoxysuccinic acid and polyaspartic acid on scaling inhibition by static and rapid controlled precipitation methods. *Desalination* **2012**, *304*, 1–10. [CrossRef]
18. Popov, K.; Rudakova, G.; Larchenko, V.; Tusheva, M.; Afanas'eva, E.; Kombarova, S.; Kamagurov, S.; Kovaleva, N. A comparative performance ranking of some phosphonates and environmentally friendly polymers on $CaCO_3$ scaling inhibition by NACE protocol. *Desalination Water Treat.* **2017**, *69*, 163–172. [CrossRef]
19. Yan, J.; Tan, X.; Qi, S. High-Temperature-Resistant Scale Inhibitor Polyaspartic Acid-Prolineamide for Inhibiting $CaCO_3$ Scale in Geothermal Water and Speculation of Scale Inhibition Mechanism. *Water* **2023**, *15*, 1457. [CrossRef]
20. Huang, H.; Yao, Q.; Jiao, Q.; Liu, B.; Chen, H. Polyepoxysuccinic acid with hyper-branched structure as an environmentally friendly scale inhibitor and its scale inhibition mechanism. *J. Saudi Chem. Soc.* **2019**, *23*, 61–74. [CrossRef]
21. Shen, Z.; Zhi, X.; Zhang, P. Preparation of fluorescent polyaspartic acid and evaluation of its scale inhibition for $CaCO_3$ and $CaSO_4$. *Polym. Adv. Technol.* **2016**, *28*, 367–372. [CrossRef]
22. Amjad, Z.; Landgraf, R.T.; Penn, J.L. Calcium sulfate dihydrate (gypsum) scale inhibition by PAA, PAPEMP, and PAA/PAPEMP blend. *Int. J. Corros. Scale Inhib.* **2014**, *3*, 35–47. [CrossRef]
23. Long, T.; Wang, Z.; Yang, W.; Yang, C.; Deng, S.; Gu, T. Effect of environmentally friendly reverse osmosis scale inhibitors on inorganic calcium carbonate scale. *Colloids Surf. A Physicochem. Eng. Asp.* **2024**, *702*, 134883. [CrossRef]
24. Ou, H.; Chiang-Hsieh, L. A synergistic effect of sodium gluconate and 2-phosphonobutane-1,2,4-tricarboxylic acid on the inhibition of $CaCO_3$ scaling formation. *Powder Technol.* **2016**, *302*, 160–167. [CrossRef]

25. Zhang, M.; Ruan, Z.; Han, Y.; Cao, Z.-W.; Zhao, L.; Xu, Y.-Q.; Cao, Z.-Y.; Shi, W.-Y.; Xu, Y. Controllable synthesis of polyaspartic acid: Studying into the chain length effect for calcium scale inhibition. *Desalination* **2024**, *570*, 117080. [CrossRef]
26. He, Z.; Zhang, L.; Wang, L.; Zhang, Q.; Luan, L. Anti-Scale Performance and Mechanism of Valonia Tannin Extract for Calcium Carbonate in Circulating Cooling Water System. *Sustainability* **2023**, *15*, 8811. [CrossRef]
27. Gil, V.; Porozhnyy, M.; Oshchepkov, M.; Ruleva, V.; Ryabova, A.; Trukhina, M.; Tkachenko, S.; Pismenskaya, N.; Popov, K. Application of fluorescent-tagged antiscalants for mitigation of membrane scaling by calcium carbonate and calcium phosphate in electrodialysis stack. *Int. J. Corros. Scale Inhib.* **2024**, *13*, 475–507.
28. Jiang, J.; Wu, Y.; He, Y.; Gao, S.; Zhang, C. Progress in Tuning of Metastable Vaterite Calcium Carbonate. *J. Inorg. Mater.* **2017**, *32*, 681–690.
29. Lyskawa, D.K.; Barbara, K.; Jakub, K. Controlling the size and morphology of precipitated calcite particles by the selection of solvent composition. *J. Cryst. Growth* **2017**, *478*, 102–110. [CrossRef]
30. Alroomi, Y.M.; Hussain, K.F. Potential kinetic model for scaling and scale inhibition mechanism. *Desalination* **2016**, *393*, 186–195. [CrossRef]
31. Sun, Y.; Gong, J.; Li, F.; Qin, W. Quantitative Methods for the Combination of Calcite, Aragonite, and Vaterite. *Chin. J. Soil Sci.* **2017**, *48*, 1069–1075.